7-23-93
E 7920

NASA Technical Memorandum 106210

On The Combustion of A Laminar Spray

Yeshayahou Levy
Technion-Israel Institute of Technology
Haifa, Israel

and

Daniel L. Bulzan
Lewis Research Center
Cleveland, Ohio

Prepared for the
Fifth International Conference on Liquid Atomization and Spray Systems – ICLASS – 91
Gaithersburg, Maryland, July 15–18, 1991

NASA

On the Combustion of A Laminar Spray

Yeshayahou Levy*
Technion-Israel Institute of Technology
Haifa 3200, Israel

and

Daniel L. Bulzan
NASA Lewis Research Center
Cleveland, Ohio 44135

ABSTRACT

A spray combustor, with flow velocities in the laminar range, exhibits a unique operating mode where large amplitude, self-induced oscillations of the flame shape occur. The phenomenon, not previously encountered, only occurs when fuel is supplied in the form of fine liquid droplets and does not occur when fuel is supplied in gaseous form. Several flow mechanisms are coupled in such a fashion as to trigger and maintain the oscillatory motion of the flame. These mechanisms include heat transfer and evaporation processes, dynamics of two-phase flows and effects of gravity (buoyancy forces). An interface volume, lying above the fuel nozzle and below the flame was found to be the most susceptible to gravity effects, and postulated to be responsible for inducing the oscillatory motion. Heptane fuel was used in the majority of the tests. Tests performed with iso-octane also showed similar results.

---

*NASA Resident Research Associate at Lewis Research Center.

INTRODUCTION

The classical paper of Burke and Schumann [1] on gaseous diffusion flames is considered a milestone in the analysis of combustion processes. Although the authors made a number of simplifying assumptions in their model, including the neglect of gravity, constant gas and air velocities, and a constant diffusion coefficient for all species, their predictions were found to show relatively good agreement with experimental measurements. Gas composition and flame dimensions were predicted at various locations above the fuel nozzle. Other researchers [2-4] followed in their footsteps and improved the original model, but always retained the assumption that the fuel was supplied in gaseous form and neglected gravitational effects.

Various observations of a Burke-Schumann type flame under laminar operating conditions revealed the phenomenon of flame tip flickering at frequencies of about 10-20 Hz. This effect, which was observed experimentally [5-9] and also predicted numerically [10, 11] is the direct result of gravity induced buoyant forces on the flow of the reaction products at some distance downstream of the nozzle, aerodynamic instabilities in the jet itself and heat release effects. Ellzey, et al. [11] presented predictions both considering and neglecting gravity. They showed that neglecting gravity gave a steady flowfield but including gravity caused large structures to form that were convected downstream at frequencies on the order of 15-20 Hz. An inviscid stability analysis for a buoyancy driven flow in an infinite candle [12] predicted the frequency of the flickering within a factor of 2. Hence, it appears that the relevance of gravity is significant for these types of flames.

Some work has been previously reported for laminar flames using fuel supplied as a liquid. A theoretical and experimental study [13] of a laminar diffusion spray flame did not encounter instabilities in the flame. Gravity was considered in this model, however, the model was derived only for steady-state conditions and consequently no instabilities were predicted. In addition, the liquid fuel was supplied directly from a nozzle as a conical spray that was surrounded by the combustion air, which is different from the Burke-Schumann configuration.

Studies by Greenberg [14-16] investigated the effects of fuel supplied as a liquid on the behavior of laminar diffusion flames in the Burke-Schumann configuration. In these studies, the central gaseous fuel jet used in the original formulation was replaced by liquid fuel droplets of various diameters carried by a flow of nitrogen. Effects of various initial velocity distributions and injection angles for the droplets were investigated. The effect of pre-evaporation of the liquid fuel droplets was also investigated. However, gravity was not included in these studies, and no instabilities in the flame behavior were predicted. An unsteady behavior of the flame was predicted [17], when gravity was neglected in the formulation, only when the fuel was supplied in a cosinusoidally alternating fashion of liquid and gas.

The present experimental study was motivated by the analytical study of Greenberg [14-15] and Greenberg and Cohen [16-17]. The objective of the present study was to experimentally investigate the effects of fuel droplet diameter, pre-evaporation of the liquid fuel and droplet trajectories on the structure of the flame in a Burke-Schumann configuration. The combustor utilized for the present study was a coaxial flow system flowing in the upward direction. The inner stream (fuel stream) contains fuel in the form of liquid droplets and fuel vapor in different proportions. The fuel was carried in the upward direction by a nitrogen gas stream. Air flowed in the outer coflowing stream. Both the fuel and air streams had equal average velocities.

EXPERIMENTAL APPARATUS

Combustor

The combustor was designed to study laminar spray combustion in an extension of the classical Burke-Schumann diffusion flame configuration. A schematic drawing of the combustor is illustrated in figure 1. The combustor consisted of two coaxial tubes. The outer tube was quartz and had an I.D. of 71 mm. Two different inner tubes were utilized in the present study. A quartz inner tube was used for internal laser diagnostics, and had an I.D. of 12.90 mm and an O.D. of 14.80 mm. A stainless steel tube with an I.D. of 12.54 mm and an O.D. of 15.80 mm was also used in the study when laser diagnostics were not required. The stainless steel tube had an electrical resistance heater attached to the outside of the tube to preheat the fuel stream for the optional case of additional pre-evaporation of the liquid fuel before it entered the combustion zone. The length (height) of the outer tube was 30 cm. Tests with 100 cm and 10 cm length tubes or even without the outer tube, were performed to eliminate the possibility of acoustic coupling effects and showed negligible differences in behavior. As illustrated in figure 1, the combustion air entered through four radial entrance holes and passed through a series of fine-mesh screens and flow straighteners. The upstream length from the screens to the combustor (the tip of the center tube) was about 25 cm and the total length of the center tube (from the atomizer to the tip) was about 50 cm.

Fuel was introduced into the combustor through the center tube in the form of fine droplets. A slightly modified Sonotek ultrasonic nozzle # 8700-60 MS or a self-assembled ultrasonic unit were used to generate the droplets. As shown in figure 2, the droplets were injected upwards as a conical spray. The droplets were then carried upwards by a nitrogen gas stream. The nitrogen was injected through a tube which surrounds the "horn" of the ultrasonic atomizer. As the droplets traveled upwards through the 50 cm tube, they partially vaporized and interacted with each other, causing a subsequent change in their size and momentum. The small droplets were carried upwards at a velocity proportional to the difference between the nitrogen carrier gas flow and their Stokes velocity. The small droplets will move at a velocity close to the velocity of the carrier gas whereas the large droplets will move at a reduced velocity. This is illustrated in figure 3. Figure 3 presents centerline phase/Doppler data taken at two axial locations of 300 mm below and at the exit of the center tube. Results are presented for droplet velocity and normalized drop number for droplet diameters up to 60 microns. Flowrates of the nitrogen and fuel streams were 13.2 x 10^{-6} and 12.0 x 10^{-6} kg/s, respectively. At both axial locations, the larger drops had lower measured velocities. The very large droplets, with Stokes velocities larger than the local instantaneous vertical velocity, will decelerate and eventually fall back. For accurate numerical predictions of droplet velocities within the fuel stream, effects of droplet collisions, coalescence, and momentum transfer need to be considered due to the very large number density of the droplets in the fuel stream.

Figure 4 presents velocity profiles for three drop sizes across the center tube at 20 mm upstream of the center tube exit at nearly the same conditions as figure 3. Flowrates of the nitrogen and fuel streams were 13.2 x 10^{-6} and 14.0 x 10^{-6} kg/s respectively. The nearly parabolic velocity profile across the tube, (see fig. 4), will cause the descending heavy droplets to move gradually radially outward to regions of lower and lower velocities until they eventually hit the wall, deform into a liquid film and flow downwards. Hence it is seen that although the flow has a Reynolds number of less than 50 and should be strictly laminar, it acquires a radial velocity component from the droplets and also turbulence as the flow moves upwards in the center tube. The number of droplets that hit the wall and the resulting flow in the downward direction was significant, especially in the lower part of the center tube. A drain was incorporated in the combustor configuration at the bottom of the center tube for continuous removal of the liquid film. The measurement of the actual fuel flow rate to the combustion zone always considered the drained amount.

The use of the ultrasonic atomization technique resulted in very low droplet injection velocities, on the order of a few cm/s, compared to m/s for conventional pressure atomizers. The mean droplet SMD diameter at the Sonotek nozzle exit was about 25 microns, depending on the operating conditions. The self-assembled atomizer was similar to an ultrasonic humidifier. A piezo-electric crystal was mounted at the bottom of a small liquid pool. When the crystal was energized (1.6 MHz, 100 Volts, peak-peak), tiny droplets were ejected from the liquid surface. Compared to the Sonotek nozzle, the self-assembled atomizer produced much larger quantities of droplets with smaller mean diameters. The measured SMD was on the order of 7-10 microns. Heptane fuel was used for the majority of the tests. Tests were also performed with iso-octane.

<u>Instrumentation</u>

Experimental measurements were obtained using two techniques. These included a two-component phase/Doppler particle analyzer (PDPA), which simultaneously measured the size and velocity of individual droplets, and a CCD camera coupled with laser light-sheet illumination for large scale observations of the two-phase flow and flame geometry.

The PDPA uses a rotating diffraction grating (RDG) to allow for frequency shifting, an option required whenever negative velocities are measured. For the present experimental configuration the relevant potential source for error in the size measurements originates from its apparent dependence on the specific trajectory of the measured droplet within the control volume and from the optical effect of the wall of the external tube. The integrated error in drop size measurement was evaluated to be less than ± 6.5%. For velocity measurements, in addition to the usual sources of error [18], the effect of the RDG operating at very low values of frequency shift was specifically investigated, due to instabilities in slow rotational velocities. The associated additional error in the measured fluctuating velocity was found to be as large as 0.0060 m/s. It should be noted that due to the relatively large number of velocity measurements obtained at each point (about 5000-10,000) and the random nature of the RDG instability, the mean velocity values were recorded to be better than 0.5% accurate. However, the relatively large error associated with the measured fluctuating velocity made it impossible to obtain accurate measurements of this quantity.

RESULTS AND DISCUSSION

The oscillatory motion encountered in the present study is different from any reported previously in the literature. In this study, the entire volume of the flame was affected in an expansion/contraction type of modulation, whereas previously reported flame flickering affected the flow of reaction products only at distances downstream of the nozzle.

Two sets of pictures are presented in figures 5(a-n) and 6(a-n). Figure 5(a-n) illustrates the flame in a typical cycle of the phenomenon displayed in a complete view of the combustor and flame. The outer quartz tube and the inner stainless center tube are clearly visible. The flame is indicated by a blue color with a glowing soot tip. Flowrates of the air, nitrogen and fuel streams were 107 x 10^{-6}, 10.1 x 10^{-6}, and 2.84 x 10^{-6} kg/s, respectively. Pictures are marked by a video clock running at 30 Hz, hence each clock increment corresponds to 33.3 ms. For example the specific flame shown has an amplitude ratio of about 1:11 and a frequency of about 3 Hz. A closer view of the phenomena is given in figure 6(a-n) where the camera was focused to image closer to the exit of the center tube containing the fuel droplets and nitrogen. In this figure, the flowrates of the air, nitrogen, and fuel streams were 119 x 10^{-6}, 11.8 x 10^{-6}, and 13.5 x 10^{-6} kg/s, respectively. It is evident that the equivalence ratio in figure 6 is much larger than in figure 5, however the basic phenomena remained essentially identical except for absolute flame dimensions and frequency of oscillation. For flow visualization, the coflow air stream was seeded with aluminum-oxide particles with a nominal size of 1 micron. The complete flowfield was illuminated by a light-sheet (from left to right in the pictures) from an Ar^+ laser. The particles observed close to the center tube tip are the fuel droplets since the nitrogen stream was not seeded. The center tube was transparent quartz in order to provide optical access. The high-intensity illumination from the laser masks the blue flame color, however, the sooting tip is still clearly evident. As previously discussed, the flow conditions in figure 6 are not identical to those in figure 5; consequently, the frequency shown here is slightly lower and about 2.5 Hz.

Except for two extreme cases of either very low velocities (up to about 1-2 cm/sec) or relatively high velocities (above about 30 cm/sec) the flame always exhibited an oscillatory motion when the fuel was supplied as a liquid. Both the flame dimensions and the frequency of the oscillations varied depending on the upstream flow conditions and ranged from 1-5 Hz for the frequency and 1:20 in amplitude ratio for the flame dimensions.

Following many sets of such photographs and local instantaneous size and velocity measurements performed with the phase/Doppler system, it is possible to establish a preliminary description of the phenomena.

The oscillatory motion of the flame appears to originate from several coupled thermal and fluid mechanic mechanisms. At each part of the flame oscillation cycle, different mechanisms are dominant, hence it seems that most of the combustion associated processes are involved in the complete cycle of the present phenomena. The relevant processes involved include molecular diffusion, heat transfer by radiation, convection and conduction, effects of gravity and bouyant forces, dynamics of two-phase flow, flow around a bluff body, and fuel vaporization effects.

A preliminary descriptive explanation of the mechanism and sequence of events within a cycle is proposed in the following:

1. At the start of the cycle, before combustion commences, the fuel stream containing nitrogen, fuel droplets and fuel vapor flows upward in the center tube until it reaches the top of the center tube. After it emerges from the center tube, the fuel stream immediately flows radially outward and downward creating a mushroom shaped cloud of nitrogen, fuel droplets and vapor. This is due to the significant density difference between the fuel stream and the surrounding co-flowing air.
2. Ignition by a descending flame initiates the reaction between the fuel vapor and the adjacent oxygen (see figs. 5 b and 6 a).
3. After ignition, the flame initially expands predominately in the radial direction at a velocity nearly equal to the flame speed (see figs. 5 c-d amd 6 b-c), consuming the fuel vapor that exists at the interface between the top of the fuel stream and the coflow air.

Thereafter, the flame spreads only in the vertical direction and the rate is now controlled by the evaporation rate of the fuel droplets (see figs. 5 e-j and 6 d-i).

4. Buoyancy effects lift the reaction products and, at a different rate, the emerging fuel stream. The fuel stream which originally flowed radially outward and downward after emerging from the center tube now acquires a positive vertical velocity component (see fig. 6 d-i). This is due to heat transfer to the fuel stream by conduction, radiation, and momentum transfer from the surrounding coflow. The height above the center tube that the fuel stream reaches appears to be a critical parameter in the dynamics of the flame.

5. Oxygen is available for reaction from two sources. The first source is radial diffusion inward from the surrounding coflow. This diffusion process must overcome the radial outward velocity of the newly generated reaction products and is probably of secondary importance. Oxygen is also available from a portion of the air stream that manages to penetrate the combustion zone from the bottom of the flame, close to the center tube lip (see fig. 6 c-j). The flow of oxygen is visualized by the seeding particles in the outside air stream.

6. The fuel is consumed primarily from the top section of the emerging fuel stream, causing a reduction in its radial dimension. This rapid reduction in the radial dimension induces a short swirling motion (see fig. 6 h-i), probably due to a temporal instability in the flow (see fig. 6 h).

7. As the fuel continues to be consumed, the flame contour undergoes a reduction both in diameter and height (see figs. 5 j-e and 6 j-l). Most of the flame length reduction appears to occur from the top, however the lower part also shrinks slightly.

8. The reduction in the flame size reduces the amount of heat transferred to the emerging fuel stream. Consequently, the fuel stream temperature is reduced causing a decrease in the velocity in the vertical direction until negative values are observed. A separation between the ascending flame and the top of the decelerating fuel stream develops which prevents a fresh supply of fuel vapor from reaching the flame (see fig. 6 k-l).

9. The coflowing air now faces a semi-rigid center bluff body consisting of the heavily droplet-laden fuel stream. The relative velocity between the coflow air and this bluff body increases due to the negative velocity at the top of the descending fuel stream. A toroidal recirculation zone is formed in the wake of the descending fuel stream with its center moving downwards (see fig. 6 l-m).

10. This toroidal recirculation increases the radial spreading of the fuel stream top (see fig. 6 n), reduces the position of the flame due to the reduced pressure at its center, and transfers some fuel vapor from the top of the fuel stream upwards due to the positive vertical velocity at the outer edge.

11. The small flame that is moved downward by the center of the toroidal vortex is sustained during this movement by the mixture of air and fuel vapor transported by the toroidal vortex (see fig. 6 l-m).

12. As the flame moves downward, it approaches the top of the emerging fuel stream in the form of a mushroom-shaped cloud described above. The fuel stream contains a large quantity of fuel vapor from vaporization of the droplets. The flame then expands rapidly in the radial direction. The vertical expansion is somewhat delayed since the flow must reverse direction from its downward movement to vertically upwards (see fig 6 m-n).

13. As the flame expands, the sequence of events repeats itself from step #3.

Hence, it appears that the modulation in the flame shape originates from the coupling between the flame and the fuel source. Although the fuel is supplied through the center tube in a steady fashion, confirmed experimentally with phase/Doppler measurements near the tip of the center tube, the region between the tip of the center tube and the bottom of the flame is sufficient to allow for the fuel stream to periodically expand vertically and collapse radially, thus inducing the unique oscillatory motion observed. This phenomenon is altogether different from the flame flickering previously reported in the literature due to the large toroidal vortices generated by the buoyantly induced flow.

As previously discussed, at very low velocities, no oscillatory motion was encountered. In this case, the carrier gas velocity was sufficient to carry only the very small droplets, while the larger ones accumulated on the inner wall and drained out of the system. Because the small droplets evaporated almost completely prior to their entrance into the combustion zone, the fuel was essentially supplied in gaseous form and stable combustion was achieved. At the other extreme, higher velocities on the order of the laminar flame speed (about 0.4 m/s for the Heptane), also established a quasi-steady flame. For this case nearly all the generated droplets were carried upwards to the combustion zone. The resulting flame height was relatively constant with some random oscillations of smaller amplitudes and at higher frequencies. At the higher flowrates, the increased momentum of the coflow air stream prevented the collapse of the inner fuel stream as it emerged from the center tube. This increased the height above the center tube that the fuel stream reached providing increased residence time for droplet evaporation to occur.

The higher velocities also increased the mixing of fuel vapor and air. In addition, at the higher velocities, a region of low velocity was formed in the wake of the central fuel stream that served to stabilize the flame. These phenomena were observed using laser light-sheet illumination of the flowfield.

CONCLUSIONS

A self-induced and continuous oscillatory motion, observed in liquid spray combustion with low velocities, is described. This phenomenon was observed over a relatively wide range of operating conditions and practically excludes the possibility of achieving laminar conditions in similar configurations.

A partially stable spray flame was achieved only at relatively high velocities where some turbulence in the flame structure was observed. A stable flame was also observed at extremely low velocities, but all droplets had vaporized by the time they reached the combustion zone. A preliminary descriptive explanation of the processes involved and supporting evidence are given. More work is currently underway in an attempt to better understand the phenomena.

The experimental techniques utilized in the present study were found to be extremely useful in obtaining insight into the phenomena governing the physical processes.

REFERENCES

1. Burke S. P., and Schumann, T. E. W. *Ind. Eng. Chem.* 20:998-1004 (1928).
2. Clarke, J. F. *Inst. Math. Appl.* 3:347-361 (1967).

3. Clark, J. F. *Proc. R. Soc. A.* 307:283-302 (1968).

4. Chung, S. H., and Law, C. K. *Combust. Sci. Technol.* 37:21-46 (1984).

5. Durao, D. F. G., and Whitelaw, J. H. *Proc. R. Soc. A.* 338:479-501 (1974).

6. Toong, T. Y., Salant, R. F., Stopford, J. M. and Anderson, G. Y. *Tenth Symposium (International) on Combustion*, The Combustion Institute, Pittsburgh, 1965, p. 1301.

7. Kimura, I. *Tenth Symposium (International) on Combustion*, The Combustion Institute, Pittsburgh, 1965, p. 1295.

8. Ballantyne, A., and Bray, K. N. C. *Sixteenth Symposium (International) on Combustion*, The Combustion Institute, Pittsburgh, 1976, p. 777-787.

9. Chen L. D., Seaba J. P., Roqumore W. M., and Goss S.P. *Twenty-Second Sumposium (International) on Combustion*, The Combustion Institute, Pittsburgh, 1988, p. 677.

10. Davis R. W., Moore E. F., Roquemore W. M., and Chen L. D. *Combust. Flame* 83:263-270 (1991).

11. Ellzey J. L., Laskey K. J., and Oran E.S. *Combust. Flame* 84:249-264 (1991).

12. Buckmaster J., and Peters N. *Twenty-First Symposium (International) on Combustion*, The Combustion Institute, Pittsburgh, 1986, p. 1829.

13. Moore J. G., and Moore J. *Sixteenth Symposium (International) on Combustion*, The Combustion Institute, Pittsburgh, 1976, p. 1123.

14. Greenberg J. B. *Combust. Sci. Technol.* 75:13-30 (1991).

15. Greenberg J. B. *Combust. Flame* 77:229-240 (1989).

16. Greenberg, J.B., and Cohen, R., "Spatial Distortion of Spray Diffusion Flames," *Atomiz. and Sprays*, Vol. 2, No. 3, pp. 275-293, 1992.

17. Greenberg, J.B., and Cohen, R., "Temporal Fluctuations of a Spray Diffusion Flame," Winter Ann. Mtg. of ASME on Heat and Mass Transfer in Spray Systems, Atlanta, GA. HTD 187, pp. 11-17, 1991.

18. Durst F., Melling A., and Whitelaw J.H. *Principle and Practice of Laser Dopler Anemometry*, 2nd ed., Academic Press, London, 1981.

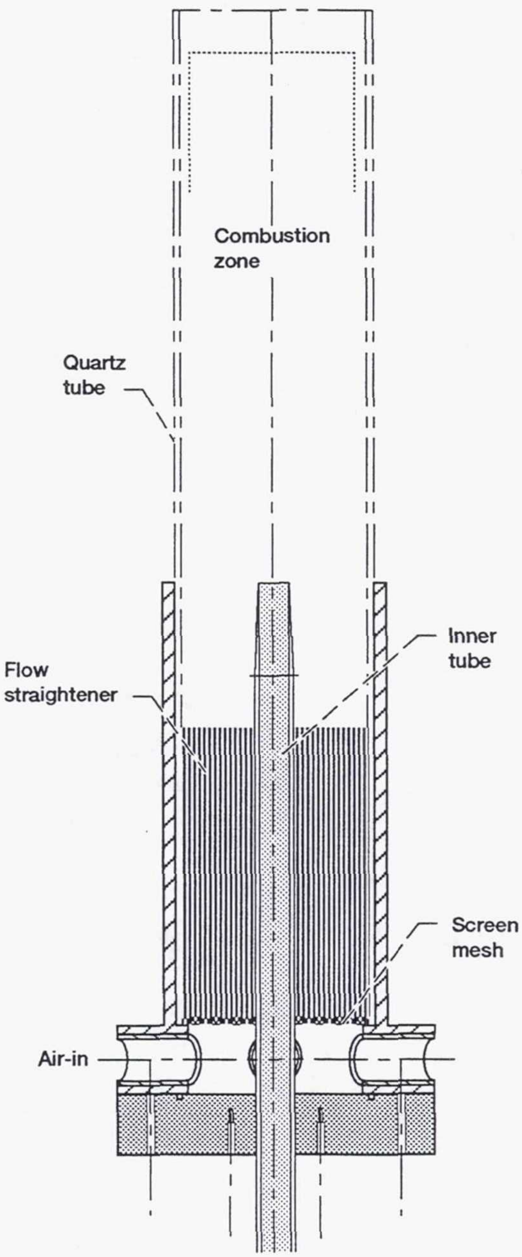

Figure 1.—Schematic drawing of the combustor.

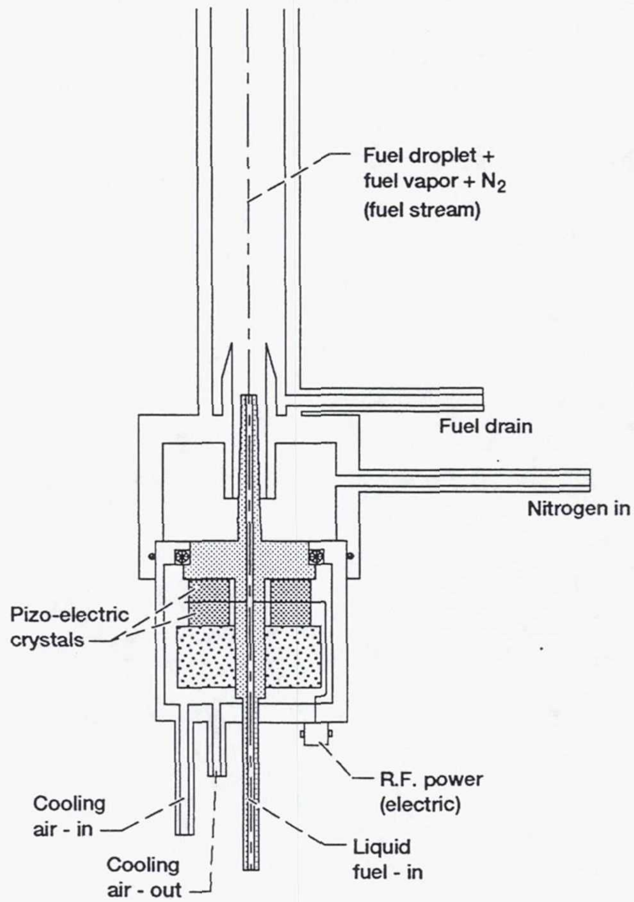

Figure 2.—Schematic drawing of the ultrasonic atomizer.

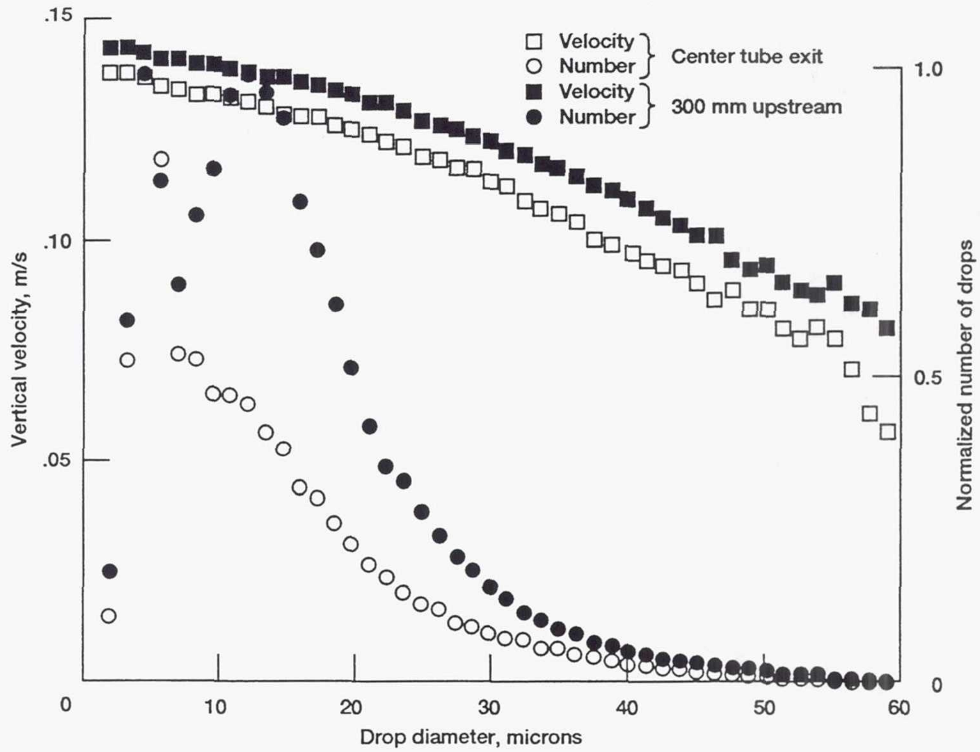

Figure 3.—Variation of centerline vertical velocity and number density with drop size at two axial locations inside the center tube.

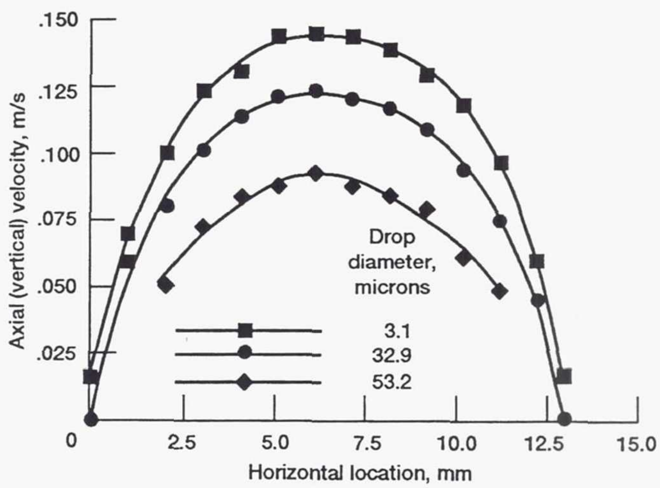

Figure 4.—Radial distribution of vertical velocity 20 mm upstream of the center tube exit.

Page intentionally left blank

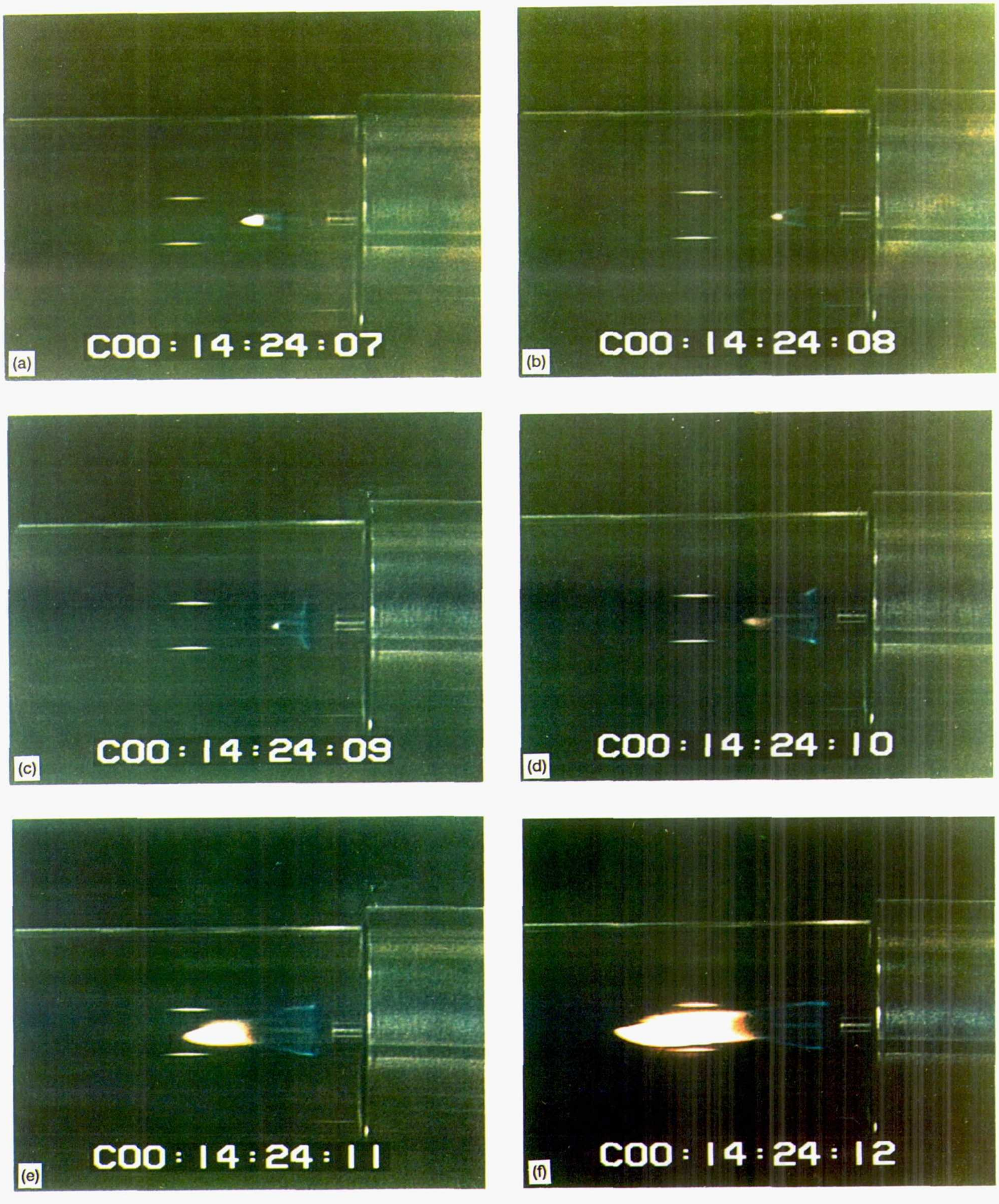

Figure 5.—Complete cycle of flame phenomenon.

Page intentionally left blank

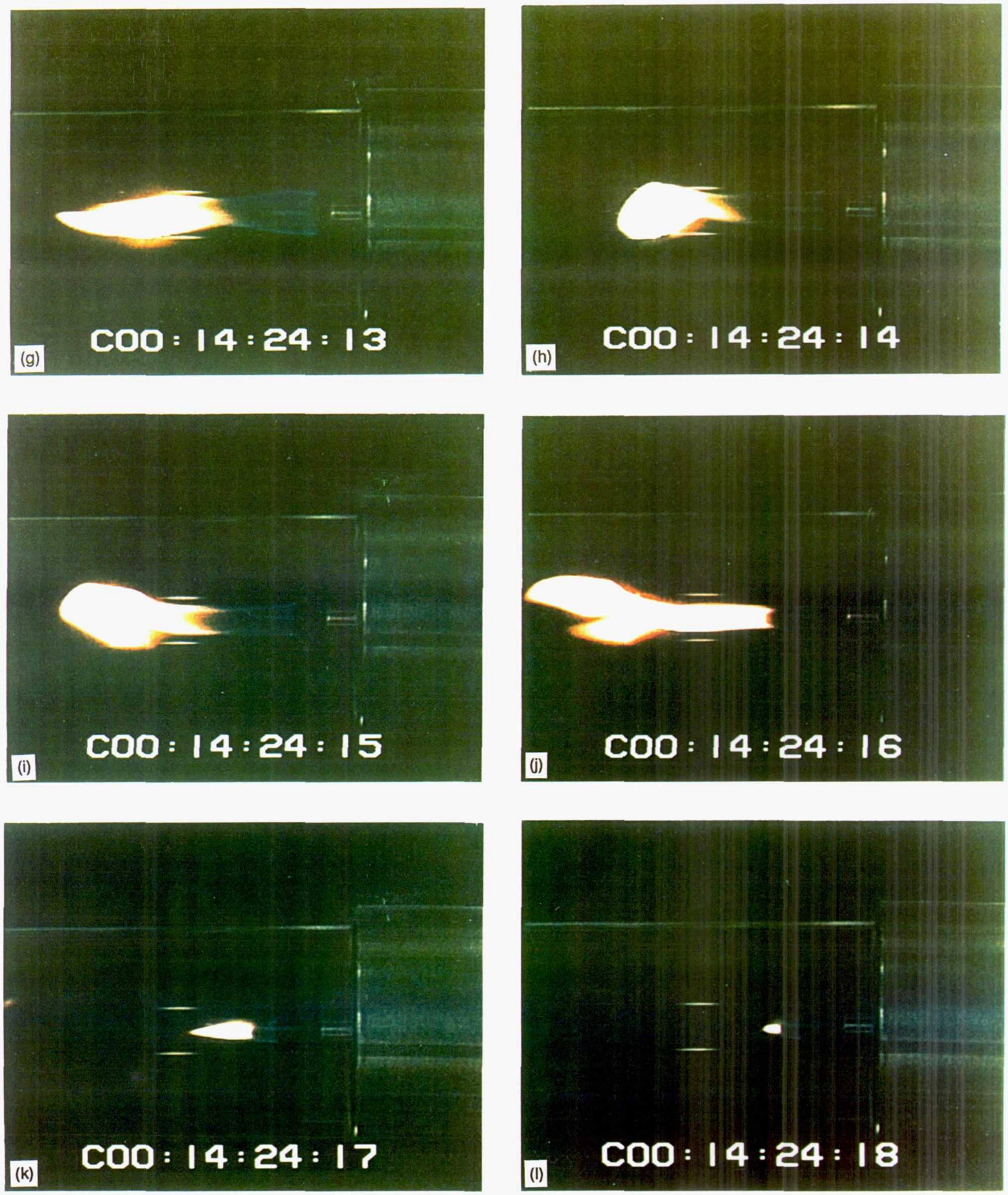

Figure 5.—Continued.

Page intentionally left blank

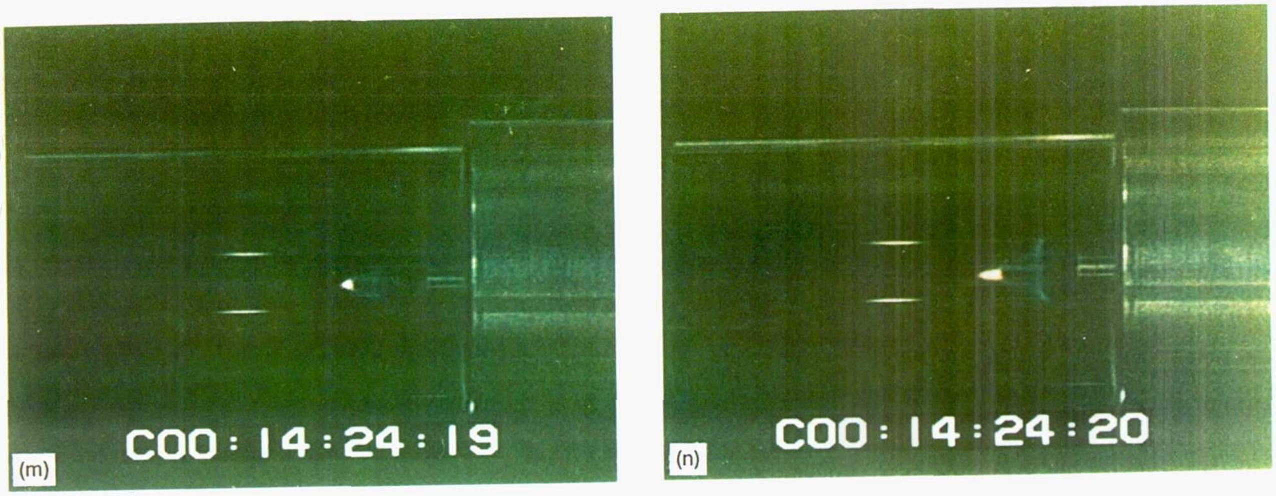

Figure 5.—Concluded.

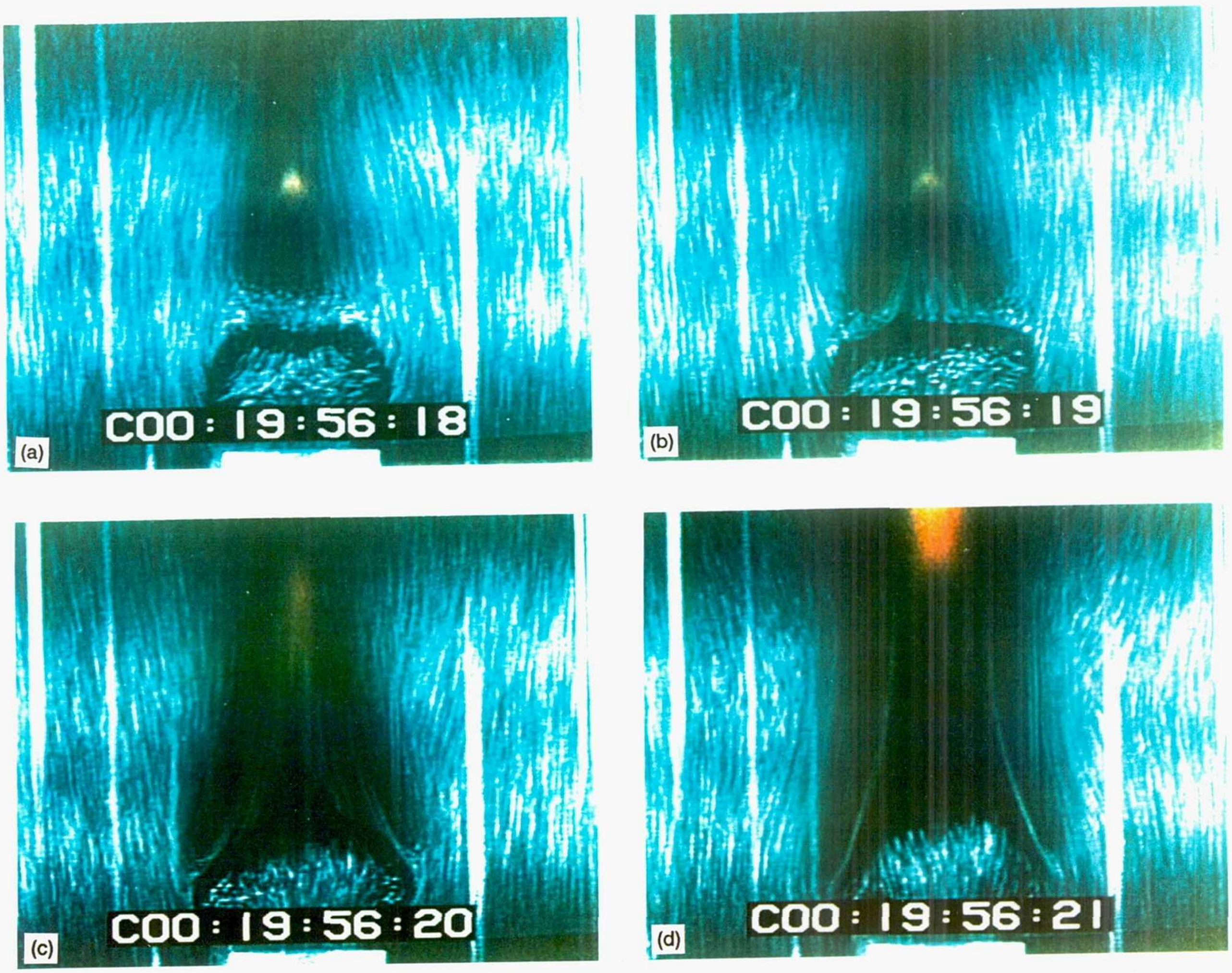

Figure 6.—Closeup view of flame phenomenon cycle with laser-sheet illumination and coflow air stream seeded.

Page intentionally left blank

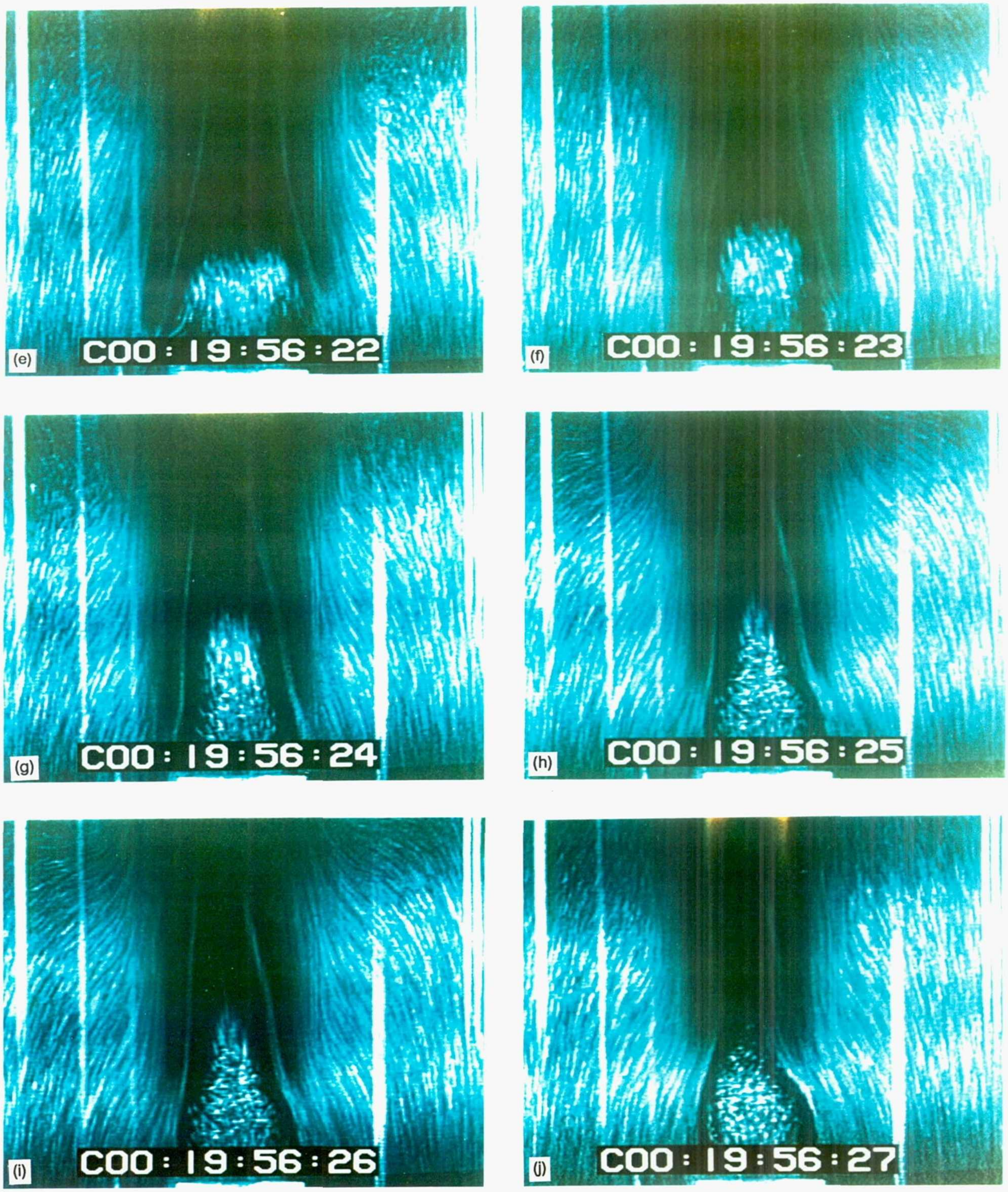

Figure 6.—Continued.

Page intentionally left blank

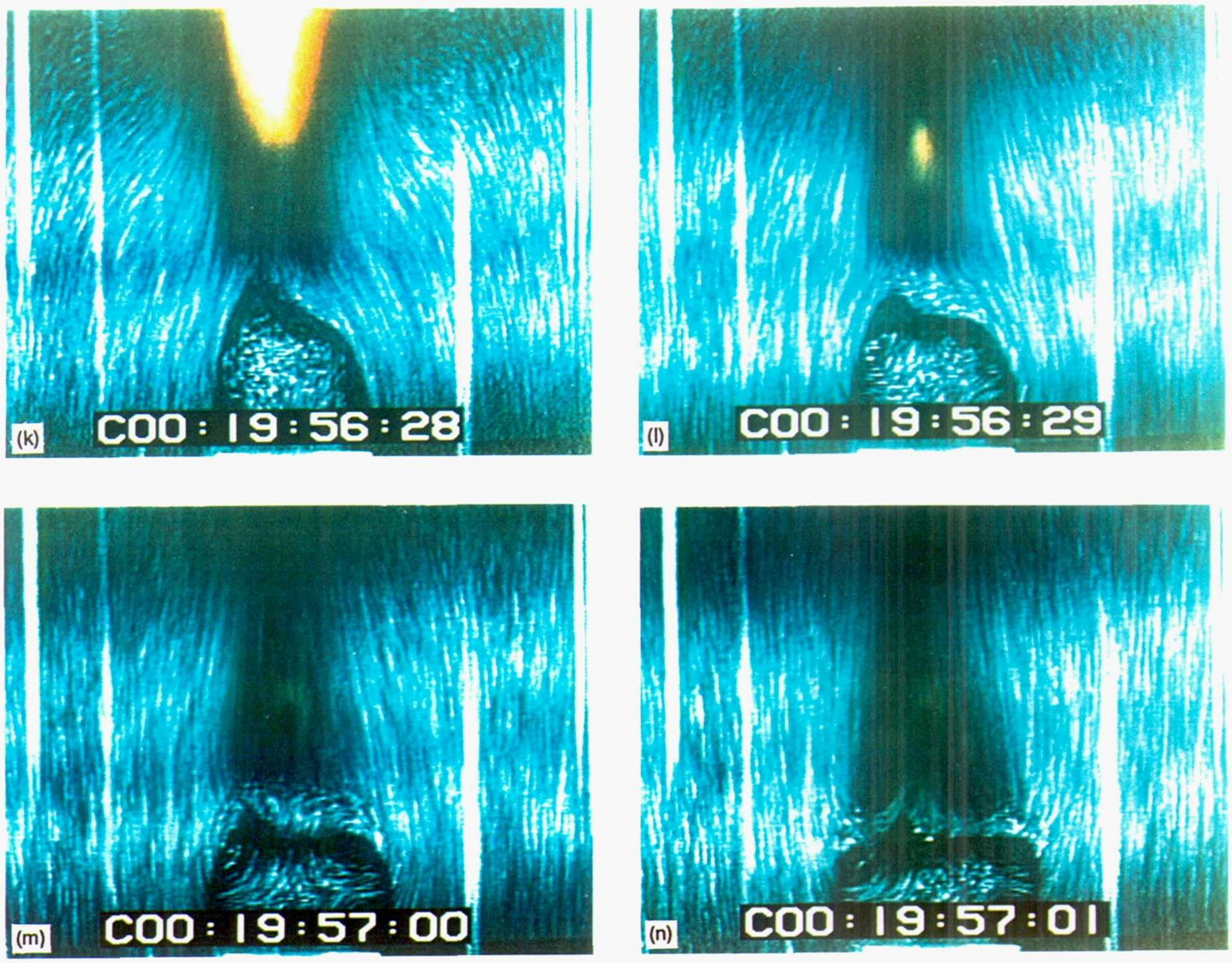

Figure 6.—Concluded.

REPORT DOCUMENTATION PAGE

Form Approved
OMB No. 0704-0188

1. AGENCY USE ONLY (*Leave blank*)	2. REPORT DATE	3. REPORT TYPE AND DATES COVERED
	July 1993	Technical Memorandum

4. TITLE AND SUBTITLE

On The Combustion of A Laminar Spray

5. FUNDING NUMBERS

WU–505–62–11

6. AUTHOR(S)

Yeshayahou Levy and Daniel L. Bulzan

7. PERFORMING ORGANIZATION NAME(S) AND ADDRESS(ES)

National Aeronautics and Space Administration
Lewis Research Center
Cleveland, Ohio 44135–3191

8. PERFORMING ORGANIZATION REPORT NUMBER

E–7920

9. SPONSORING/MONITORING AGENCY NAME(S) AND ADDRESS(ES)

National Aeronautics and Space Administration
Washington, D.C. 20546–0001

10. SPONSORING/MONITORING AGENCY REPORT NUMBER

NASA TM–106210

11. SUPPLEMENTARY NOTES

Prepared for the Fifth International Conference on Liquid Atomization and Spray System - ICLASS - 91, Gaithersburg, Maryland, July 15–18, 1991. Yeshayahou Levy, Technion-Israel Institute of Technology, Haifa 3200, Israel and NASA Resident Research Associate at Lewis Research Center and Daniel L. Bulzan, NASA Lewis Research Center, Cleveland, Ohio. Responsible person, Daniel L. Bulzan, (216) 433–5848.

12a. DISTRIBUTION/AVAILABILITY STATEMENT

Unclassified - Unlimited
Subject Category 07

12b. DISTRIBUTION CODE

13. ABSTRACT ***(Maximum 200 words)***

A spray combustor, with flow velocities in the laminar range, exhibits a unique operating mode where large amplitude, self-induced oscillations of the flame shape occur. The phenomenon, not previously encountered, only occurs when fuel is supplied in the form of fine liquid droplets and does not occur when fuel is supplied in gaseous form. Several flow mechanisms are coupled in such a fashion as to trigger and maintain the oscillatory motion of the flame. These mechanisms include heat transfer and evaporation processes, dynamics of two-phase flows and effects of gravity (buoyancy forces). An interface volume, lying above the fuel nozzle and below the flame was found to be the most susceptible to gravity effects and postulated to be responsible for inducing the oscillatory motion. Heptane fuel was used in the majority of the tests. Tests performed with iso-octane also showed similar results.

14. SUBJECT TERMS

Spray combustion; Laminar

15. NUMBER OF PAGES

29

16. PRICE CODE

A03

17. SECURITY CLASSIFICATION OF REPORT	18. SECURITY CLASSIFICATION OF THIS PAGE	19. SECURITY CLASSIFICATION OF ABSTRACT	20. LIMITATION OF ABSTRACT
Unclassified	Unclassified	Unclassified	